Iraqi Geological Journal

Journal homepage: https://www.igj-iraq.org

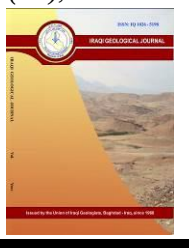

Subsurface Soil Evaluation Using 2D Electrical Resistivity Tomography for Foundation Studies at Najaf City, Iraq

Alhawraa A. Ali[1*] and Amer A. AlKhalidy[1]

1 Department of Applied Geology, College of Science, University of Babylon, Iraq
* **Correspondence**: alhawraaaqeelali@gmail.com

Received:
4 May 2025
Accepted:
4 January 2026
Published:
31 March 2026

Abstract

At two locations in Al-Najaf City, Al-Ghadeer Village and Zain Al-Abideen Street, a two-dimensional Electrical Resistivity Tomography survey was carried out using the ABEM Terra LS2 and three electrode configurations: Wenner, Schlumberger, and Dipole-Dipole. Assessing subsurface geotechnical conditions and identifying weak or abnormal zones were the goals of the study. Each array made a unique contribution to the interpretation: The Schlumberger attained deeper penetration and better vertical resolution close to the groundwater-saturated layers. The Dipole-Dipole provided the best lateral resolution for mapping possible cavity-related anomalies. Whereas the Wenner offered high signal stability and dependable detection of shallow lithological variations. According to drilling data (BH-13, BH-15, and BH-16), low resistivity anomalies (0.27–9.5 Ωm) in Al-Ghadeer Village were associated with sandy clay and localized dissolution characteristics. In Zain Al-Abideen Street, very low resistivity zones (<1.0 Ωm) beneath paved surfaces matched field-observed subsidence, indicating weak saturated soils, while deeper high-resistivity layers corresponded to dry gypsum-rich sands (BH-1). Integrating Electrical Resistivity Tomography with borehole information enhanced the interpretation confidence. The upper layers (0.5–2.5 m) are generally suitable for shallow foundations, but deeper weak zones require caution. Localized cavities likely associated with gypsum dissolution may trigger future ground collapse. The Schlumberger array gave the best vertical detail, especially at deeper depths, while the Dipole-Dipole array was more sensitive to horizontal changes. The Wenner array gave balanced results but with slightly higher RMS errors. Additional investigations such as 3D ERT imaging or geotechnical load testing are recommended, and soil improvement or deep foundations may be necessary in hazardous zones.

Keywords: Geophysical surveys; Engineering assessments; 2D electrical resistivity Tomography method

1. Introduction

Since it examines the distribution of potentials and gives a clear picture of the electrical resistivity distribution below the earth's surface, the electrical resistivity method (Telford et al., 1990) is a method that is used to ascertain the mechanical and physical characteristics of soils and shallow-depth subsurface rocks (Afuwai, 2013. The properties of the active layer, or the soil near the earth's surface, which normally contains moisture that fluctuates constantly due to weathering and climatic changes, like rainfall in the winter and evaporation in the summer, are what largely determine how buildings affect the earth's surface (Shakir et al., 2013).

The resistivity method, which entails transferring an electric current through current electrodes and measuring the voltage on potential electrodes, is the fundamental concept upon which the Electrical

Resistivity Imaging measurements are based (Nordiana et al., 2012). Over the past few decades, electrical resistivity imaging has been used extensively as a pre-excavation surveying tool in numerous near-surface engineering and environmental studies (Reynolds, 2011). Additionally, electrical resistivity has been used to determine the thickness of economically viable deposits of building materials like gravel and sand and to locate subsurface features like valleys, submerged canals, and big holes. Environmental protection and environmental science also make use of it (Kelly, 1976). One, two, or three-dimensional surveys can be carried out at a range of scales and resolutions, from extremely local to regional. Complex geological formations that were previously impossible to map using the results of conventional 1D resistivity surveys can now be mapped using 2D resistivity surveys (Dahlin, 1996).

Electrical resistivity imaging and soil analysis have been shown in a few other investigations to work together to produce continuous subsurface details and penetrate many meters deeper into the subsurface. Site planning techniques that yield the best information utilizing various ERI configurations positioned in diverse geological formations have been the subject of numerous studies (Islam et al., 2012). The study of Al-Khalidy (2025) aimed to determine the geotechnical properties of the soil at the Electrical Power Station project site in Al-Debony, Iraq by applying the Vertical Electrical Sounding (VES) technique using the Schlumberger array. It also sought to evaluate the subsurface layers and their physical and engineering properties, such as soil resistivity and layer thickness, in order to support the safe and reliable design and construction of structural foundations for the project. Mohammed et al. (2021) employed two-dimensional (2D) electrical resistivity imaging to detect subsurface voids and fractures of different shapes and sizes within gypsum rock layers. These features were interpreted as weak zones that may pose significant structural risks to government and residential buildings. Their study concluded that the karst subzone facilitates the transmission of sulfur-rich groundwater across large areas of Hit city in the western part of Iraq.

2D electrical resistivity imaging was applied to investigate groundwater conditions in the west of Ramadi city. The inverted resistivity models revealed clear variations between anomalous water-saturated zones and surrounding sediments. The maximum thickness of the saturated layer reached approximately 10.5 m, predominantly within secondary gypsum and claystone layers containing secondary gypsum and siltstone, which represent the upper lithological units of the Injana Formation, underlying the University of Anbar campus.

At a test site in Venice (Italy), electrical resistivity imaging techniques were also employed to assess the degree of restoration of the buildings' foundations following consolidation. It was found that the brick wall foundation's resistivity readings showed that there were cracks and cavities. While the intermediate resistivity values (20–100 Ωm) were correlated with good sections of the foundation, the low resistivity values (10 Ωm) were caused by the complete decomposition or destruction of the bricks, which were completely replaced by defective mud material (Abu Zeid et al., 2006). The high resistivity of the wall (> 150 Ωm) was explained.

This study examines how the 2D electrical resistivity method was used to determine the resistivity values and soil lithology for soft soils in the Al-Gadeer Village and Zain Al-Abideen region at Al-Najaf, Iraq.

2. Geology of the Study Area

Al-Najaf City is located 161 km southwest of Baghdad, the capital of Iraq, on the border between the Southern Desert in the west and Mesopotamia (Tigris and Euphrates floodplains) in the east. The terrain slopes gently in the direction of the floodplain (Shakir et al., 2013; Al-Farhan et al., 2019).

The Al-Najaf City is located between latitudes 44° 17′ 00″ and 44° 25′ 00″ East and 32° 7′ 00″ and 31° 56′ 00″ North). And 31°59'51.5"N, 44°19'07.3"E for the site Al-Sd, 32°05'08.2"N, 44°20'07.9"E for Al-Ghadeer site. Its desert environment is defined by high summer temperatures of up to 44 °C and a

low annual rainfall (102 mm) (Al-Farhan et al., 2022). Fig. 1 displays the location of Al-Najaf City and the study area on the geologic map. The region selected for this investigation is shown by the red dot that is highlighted in Fig. 1.

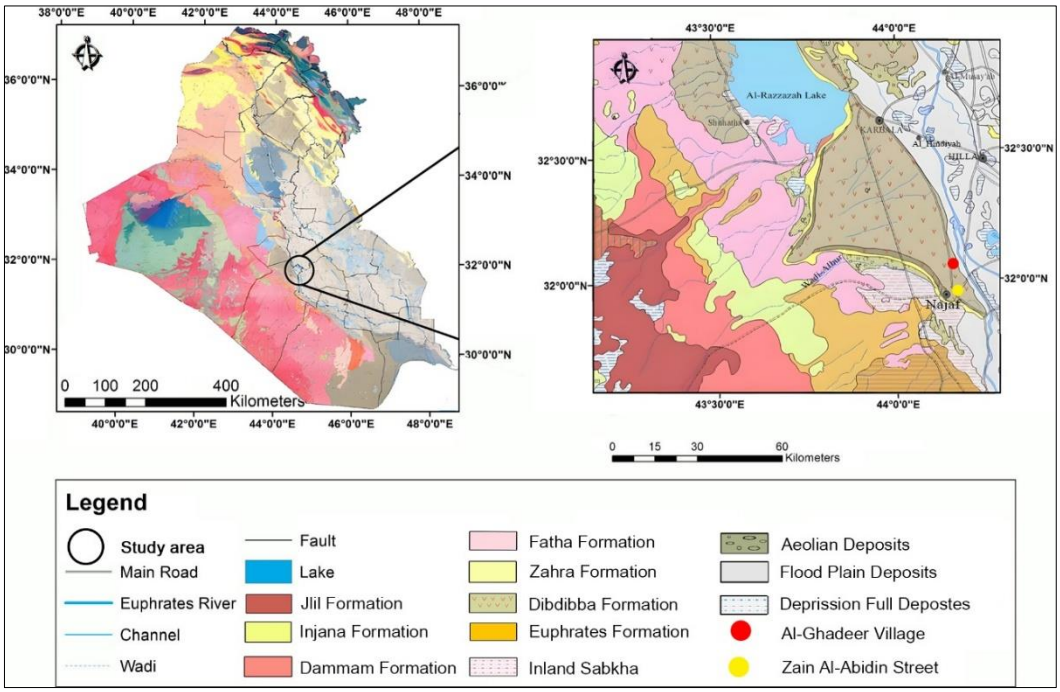

Fig. 1. Locations of the study area within the geologic map of Iraq, modified from Sissakian and Fouad (2015)

There are many different types of geological deposits in the studied area. The oldest is the Dibdibba Formation (Pliocene–Pleistocene), which is exposed west of the study area. Sandstone is the main constituent of the Dibdibba Formation. Small, poorly sorted pebbles with fine-coarse grains of sandstone are frequently described as having a thickness of roughly 10 m. The Injana Formation (Upper Miocene) underlies the Dibdibba Formation (Hussein et al., 2022). Between 20 and 35 m thick, the Injana Formation mainly consists of red, partly greenish, silty, sandy calcareous claystone and lenticels of grey, brownish, greenish, and yellowish sandstone (Awadh et al., 2024).

The sequence also occasionally contains thin beds (0.30 m) of chalky and marly limestone (Pleistocene–Holocene), which covers the Dibdibba Formation, is exposed over the majority of the study area to a thickness of 0.5–2 m of secondary gypsum in the following forms: powdery, fibrous prismatic, hard, well-crystallized, and brownish spongy. A small part of the studied area lies to the east and south of the Holocene sediments, which include floodplains and anthropogenic deposits. Loam, a mixture of clayey silt deposits from the Euphrates River, makes up the deposits of the Flood Plain and can reach a thickness of up to 1.5 m (Awadh et al., 2024).

3. Materials and Methods

3.1. Field Work and ERT Survey Equipment

The fieldwork was conducted in October 2024 at two different locations within Al-Najaf Governorate. The first location (2DG, 2 dimensions for Al-Ghadeer) is a residential complex in Al-Ghadeer Village, while the second location (2DZ) is Zain Al-Abideen Street. Both sites showed clear signs of surface subsidence. Since both locations had paved surfaces, a hammer drill was used to create small holes for the electrodes to be inserted, as it was not possible to insert them directly into the asphalt. In the first site (2DG, Al-Ghadeer Village), the survey line was 96 m long with an electrode

spacing of 4 m. The interpretation (Fig. 2) was supported by the use of data from three boreholes (BH1, BH2, and BH3) provided by Al-Mawal Engineering Company.

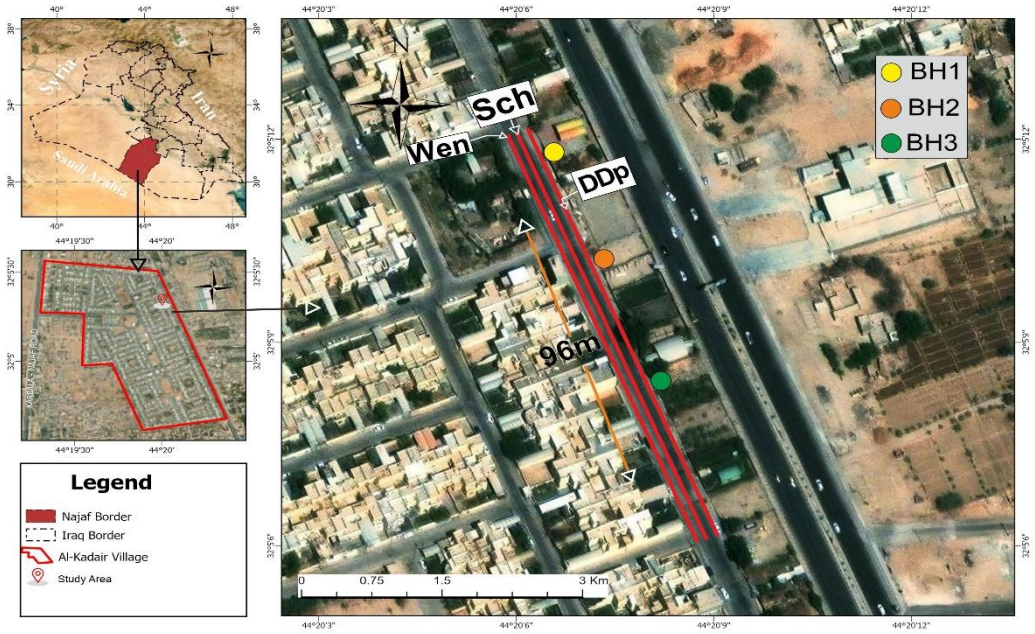

Fig. 2. Satellite image shows the first studied site (Al-Ghadeer Village) and ERT profiles locations (Schulmberger, Dipol-Diople and Wenner)

In the second site (2DZ - Zain Al-Abideen Street), the survey line was only 24 m long, with 1 m spacing between electrodes to obtain more detailed near-surface measurements. Borehole data from BH1 were used in this location (Fig. 3). Al-Mawal Engineering Investigations Company supplied us with an ABEM Terrameter LS2 device. It was connected to 24 electrodes using flexible cables arranged along the survey line. Three different electrode array configurations: Wenner, Schlumberger, and Dipole-Dipole were applied to enhance the accuracy of the results. After fixing and connecting the electrodes to the device, subsurface resistivity values (readings) were started by us. These values were stored and converted into data for further analysis. The RES2DINV software (version 4.8.12) was used to utilized two-dimensional resistivity sections that illustrate lateral and vertical variations in subsurface electrical resistivity associated with different soil lithologies.

3.2. Data Processing and Inversion

The RES2DINVx64 software was used to analyze the 2D resistivity data. This software relies on the finite difference method for forward modeling. The data collected using the three electrode configurations were processed in the same way. A damping factor of 0.3 was used for the Zain Al-Abideen site because the data was more stable, while a higher value of 0.5 was chosen for the Al-Ghadeer village site due to harder conditions and more noise. The robust inversion method was applied to reduce the effect of noisy data and get clearer results. Before the inversion, bad data points were removed manually to clean the dataset. Then, the inversion was performed to generate a resistivity model that could be easily interpreted. After several inversion attempts, the calculated values closely matched the measured values. The Root Mean Square (RMS) error was used to measure the difference between the measured and calculated values (Thabit and Al-Zubedi, 2015).

The profiles that had the lowest RMS error were chosen for the final interpretation. In Al-Ghadeer Village site, the Wenner configuration, which focuses on subsurface vertical change, the RMS error after five attempts was 16.6%, which is acceptable.

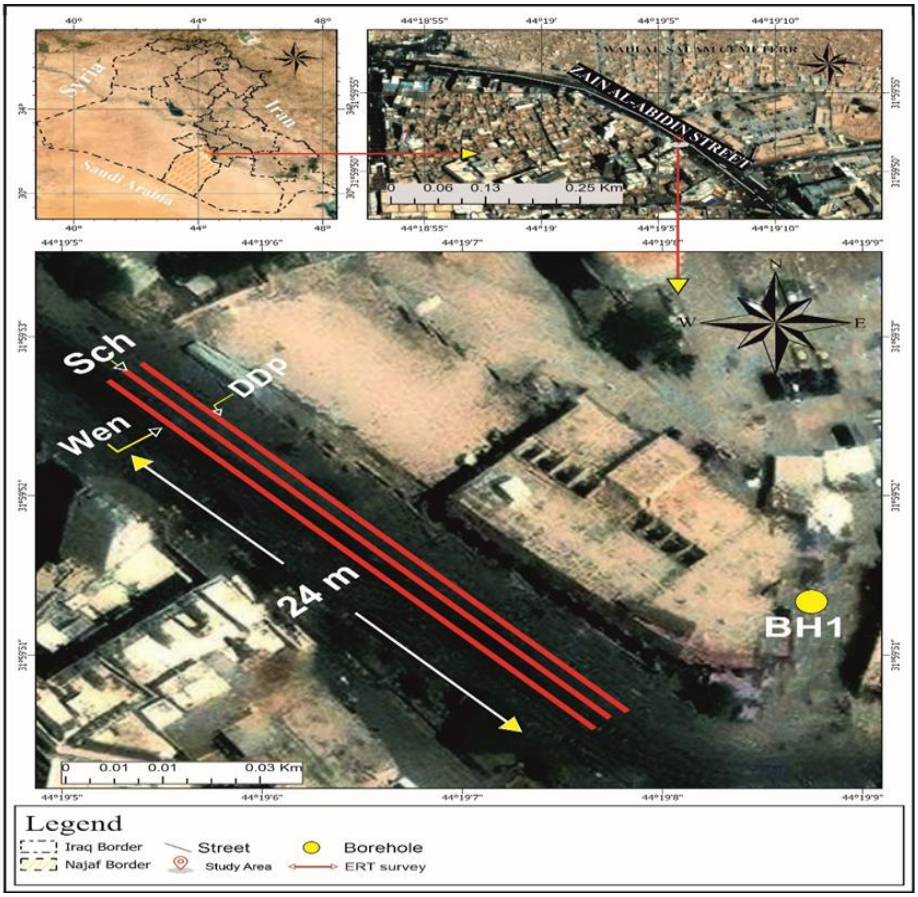

Fig. 3. The locations of the ERT profiles (identical red lines) and the second study area (Zain Al-Abideen Street) are visible in the satellite image.

In the Schlumberger configuration, which allows for better penetration, the error was 11.2%, indicating a good match between the measured and calculated data. For the Dipole-Dipole configuration, which is sensitive to horizontal changes, the error was 15.4%, which is also an acceptable value (Loke, 2021). For the Zain Al-Abideen Street site, we followed the work steps. In the Wenner configuration, the RMS error after four attempts was 10.3%. The profile showed a low-resistivity area in the middle of the section, which matches the location of the visible surface subsidence. In the Schlumberger configuration, the RMS error was 9.0%, and the profile showed a variation between the shallow and deep layers. For the Dipole-Dipole configuration, the error was 15.4%.

These interpretations were supported by data from BH1, which is located on the same survey line 1. The inverted resistivity models (Fig. 6a–c) reveal a nonhomogeneous subsurface characterized by significant lateral and vertical variations in resistivity. The blue to green hues in the top zone (0–6 m in depth) indicate low to moderate resistivity levels, which range from around 0.5–7 Ωm. This behavior is in good agreement with the borehole data (BH1), which confirms the existence of fill materials with subterranean caverns made of gypsum-containing silty sand with a high moisture content.

These conditions indicate weak soil packages; prone to settlement or collapse. Below 6 m depth, a transition to higher resistivity values (up to 20–30 Ωm and locally exceeding 30 Ωm) was observed, particularly toward the central and deeper parts of the profiles. This zone reflects a silty-sandy layer containing secondary gypsum. with fine gravel and minor clay, a relatively stronger lithological unit compared with the upper disturbed filling soil. The localized high-resistivity anomalies highlighted in red may indicate: gypsum-rich cemented zones, possible air-filled cavities or void remnants.

Meanwhile, patches of very low resistivity (<2 Ωm) at depth indicate water infiltration paths associated with karst dissolution and weakness zones. The 2D inversion for the second site is shown in Fig. 6.

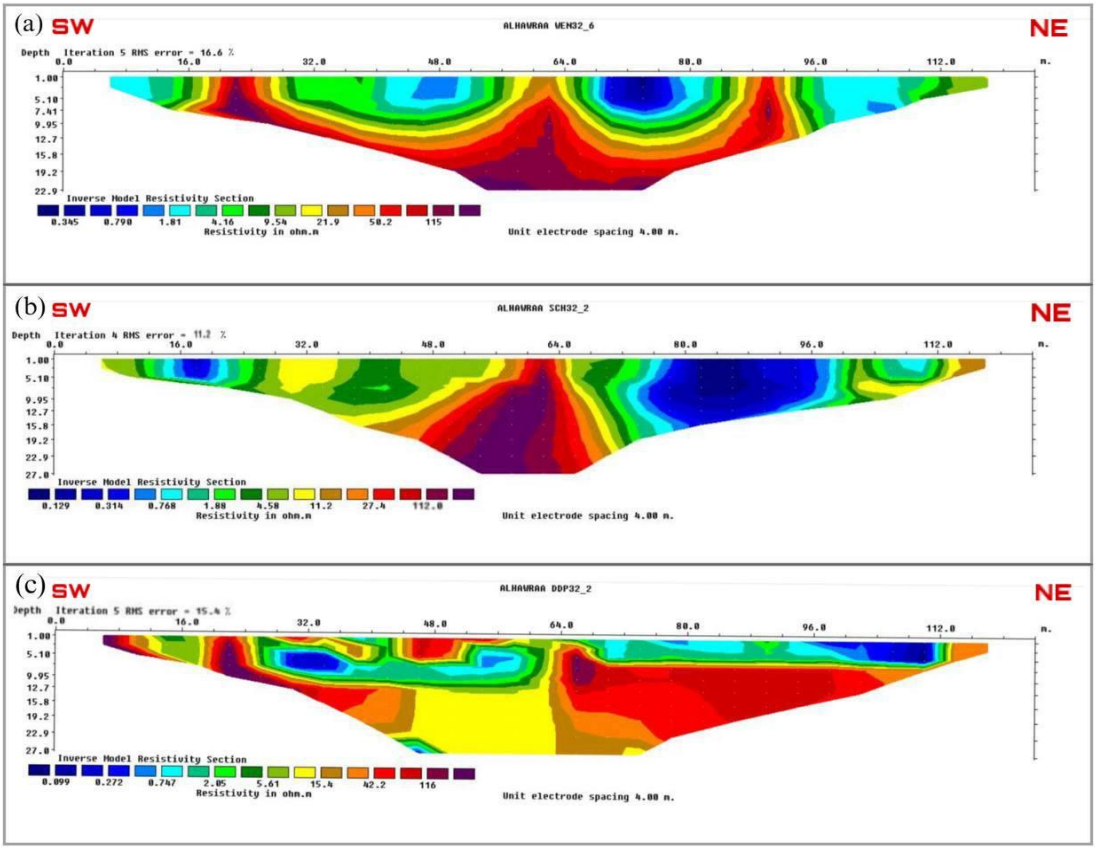

Fig. 4. 2D inversion of electrical resistivity for the three electrode arrays of 2DG site arranged as follows: Wenner (a), Schlumberger (b), and Dipole-Dipole (c), respectively

These conditions indicate weak soil packages; prone to settlement or collapse. Below 6 m depth, a transition to higher resistivity values (up to 20–30 Ωm and locally exceeding 30 Ωm) were observed, particularly toward the central and deeper parts of the profiles. This zone reflects a silty-sandy layer containing secondary gypsum. With fine gravel and minor clay, a relatively stronger lithological unit compared with the upper disturbed filling soil. The localized high-resistivity anomalies highlighted in red may indicate: gypsum-rich cemented zones, possible air-filled cavities or void remnants. Meanwhile, patches of very low resistivity (<2 Ωm) at depth indicate water infiltration paths associated with karst dissolution and weakness zones. The 2D inversion for the second site is shown in Fig. 5.

4. Results and Interpretation

4.1. Results of the Site (2DG)

4.1.1. Wenner array

The Wenner array profile was conducted from the northeast to the southwest in the study area. The depth reached by this profile is about 22.9 m. Three boreholes were used (BH-13, BH-15, and BH-16) to help match the layers with the electrical results. Also, Al-Mawal Engineering Investigations Company mentioned that the groundwater was found at a depth of 1.8 m. From the resistivity data, there are three main zones that we can observe. The first zone is shallow and starts from the ground surface to about 1.8

m in depth. It displays resistivity values between 0.79 and 9.5 Ωm, which is low to medium in Fig.6. This most likely indicates that the soil is silty sand that is either close to the water table or contains some water. The finding appears to be trustworthy since the decline in resistivity; here is consistent with the groundwater level from the boreholes.

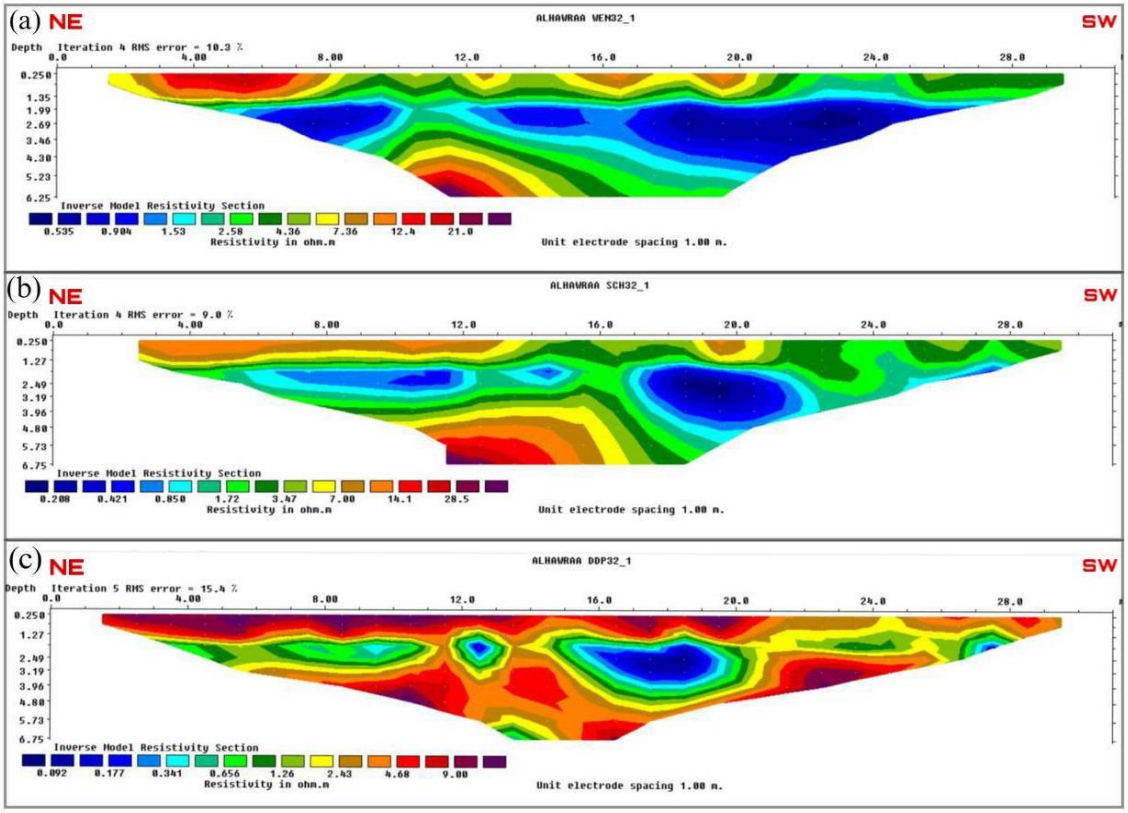

Fig. 5. 2D inversion of electrical resistivity for the three electrode arrays of (2DZ) site arranged as follows: Wenner a), Schlumberger b), and Dipole-Dipole c) respectively

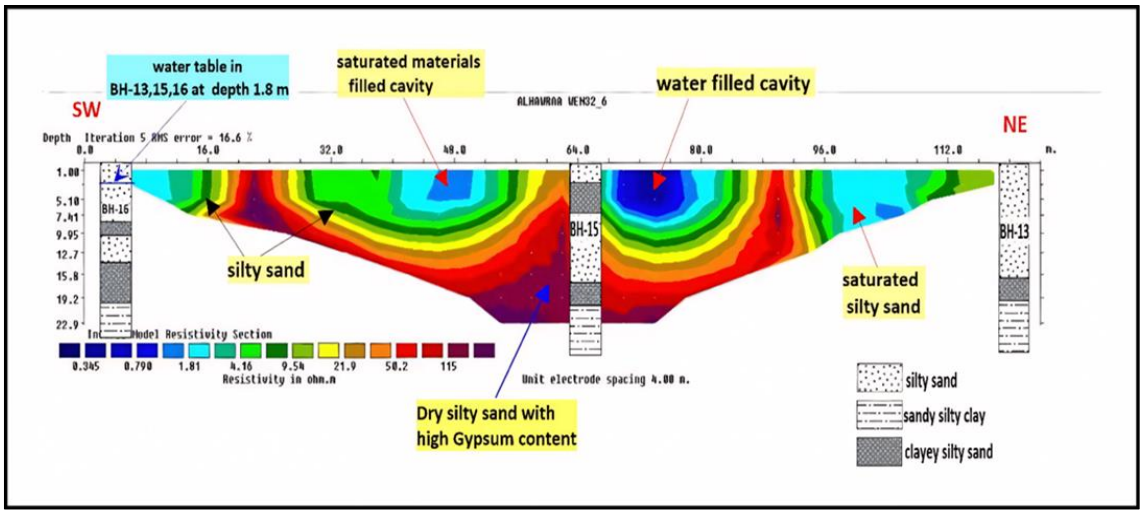

Fig. 6. Wenner array of site (2DG) inverse models of synthetic models

The depth of the second zone is from 1.8 to 15 m. Two locations in this zone exhibit extremely low resistivity (less than 1.0 Ωm). These locations may be found between BH-16 and BH-15 as well as between BH-15 and BH-13. These low values might be caused by caverns or water-filled gaps created by dissolved gypsum underneath. The low resistivity indicates that these locations are most likely

flooded, maybe with karst characteristics or fractures. Due to the potential for the ground to subside, some sites may be hazardous. The resistivity increases from 21.9 to 50 Ωm in the third zone, which is deeper than 15 m, particularly on the southwest side of the resistivity profile. This may indicate that the soil is drier and composed of gypsum-containing silty sand. This kind of soil can gradually erode over time despite its sturdy appearance.

٤.1.2. Schlumberger array

The Schlumberger profile reaches a depth of around 27 m and spans the same region as the other profiles, from southwest to northeast. Together with drill data from BH-13, BH-15, and BH-16, the resistivity results aid in our understanding of the ground's layers and any anomalous subsurface characteristics. The boreholes indicate that the groundwater level is at a depth of 1.8 m. The resistivity values are modest to high in the shallow subsurface (up to 1.8 m depth), ranging from 0.79 to 8.6 Ωm in Fig.7. This indicates that the soil is probably composed of silty sand that has been saturated with moisture or water, which is consistent with the groundwater level observed in the boreholes. This serves to verify that the resistivity model accurately depicts the location of the water table.

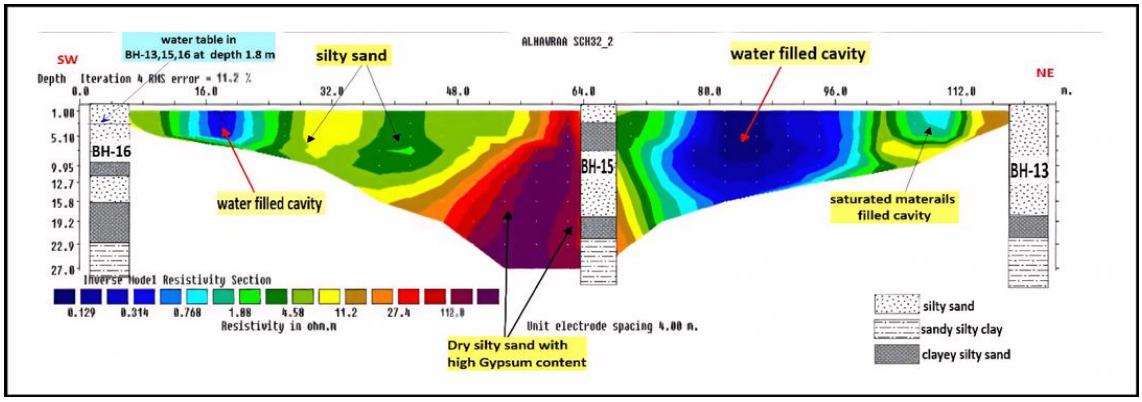

Fig. 7. Inverse models of the synthetic model for the Schlumberger array of site 2DG

Two locations with extremely low resistivity are visible between 1.8 m and roughly 14 m below the surface. These locations are interpreted as water-filled cavities or zones of gypsum dissolution, based on resistivity values below 1.0 Ωm. These characteristics may result in soil issues, such as instability or ground sinking due to these caverns. The dispersion of these anomalies implies that water may flow more readily in certain locations, thereby exacerbating the breakdown. The resistivity values increase between 19.4 and 48 Ωm for depths greater than 14 m. This indicates that the soil turns into silty sand that is drier and may include a lot of secondary gypsum. Despite the strength of these layers, the secondary gypsum can gradually disintegrate over time, particularly in the presence of groundwater, which might eventually make the soil weaker.

4.1.3. Dipole-dipole array

Borehole data from BH-13, BH-15, and BH-16 are connected to the 2D resistivity model from the Dipole-Dipole array, which spans the region from southwest to northeast. Based on data from boreholes, the groundwater level in the region is around 1.8 m. The initial layer in the southwest (near BH-16) has extremely low resistivity values (0.272–0.747 Ωm) down to a depth of around 5 m. This is consistent with the groundwater level discovered in the boreholes and points to shallow water-filled voids. The soil in this area is silty sand has been saturated with water, according to the borehole records. A moderate resistivity zone (2.05–5.61 Ωm) lies below this depth (1.8 m), which, like what was discovered in BH-16, is thought to be silty sand (Fig. 8).

The drill logs show that this stratum is generally dry with some secondary gypsum content. Another shallow cavity with very low resistivity values (0.272–0.747 Ωm) between BH-16 and BH-15 indicates another void or water-filled zone. A larger area of increased resistivity (5.61–42.2 Ωm) surrounds this location, suggesting dry silty sand with a high secondary gypsum concentration that may be connected to local evaporite deposits. Several abnormalities are found when compared with BH-15 and BH-13. Both shallow and deep voids are easily detected by the Dipole-Dipole array, which is sensitive to both vertical and horizontal resistivity variations. A notable low-resistivity zone (~0.272 Ωm) is found near the northeastern part, close to BH-13, pointing to a water-filled cavity likely formed by the secondary gypsum dissolution and collapse. Around this low-resistivity area, there are saturated silty materials with resistivity values between 0.747 and 2.05 Ωm This indicates areas that are partially saturated and structurally weak but haven't totally collapsed.

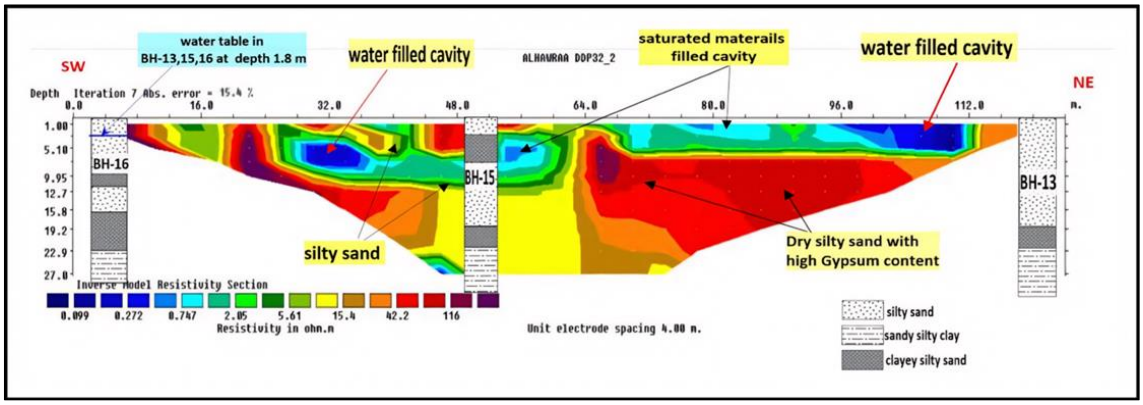

Fig. 8. Inverse models of the synthetic model for the Dipole-Dipole array of site 2DG

4.2. Result of the Site 2DZ

4.2.1. Wenner array

In the resistivity section obtained using the Wenner array, the subsurface layers show a range of resistivity values from about 0.5 to more than 21 Ωm The uppermost layer, especially on the northeastern side of the site, shows relatively high resistivity values between 7 and 12 Ωm, which is interpreted as a concrete surface layer. Below this, resistivity drops significantly between 1 and 4 Ωm, which can be seen in the middle part of the section and extends towards the southwest. These low resistivity zones indicate the presence of water-filled cavities formed by the dissolution of the secondary gypsum, which weakens the soil structure (Fig. 9).

Beneath these cavities, there are zones with resistivity values above 12 Ωm, interpreted as dry sand with high secondary gypsum content. On both sides of the section, especially towards the southwest, moderately low resistivity values suggest the presence of wet silty sand. The near-surface areas above these zones, on the other hand, have an increased resistivity, which is consistent with dry silty sand. Although it was marginally less sensitive to lateral shifts close to the surface than the Dipole-Dipole array, the Wenner array generally produced a balanced image with high vertical resolution, making it useful for distinguishing the layered structure and deeper details.

4.2.2. Schlumberger array

The resistivity values in the resistivity section acquired with the Schlumberger array varied from 0.2 to more than 28 Ωm. Variations in the underlying layers are evident in these values. Low resistivity zones (between 0.2 and 1.7 Ωm) appeared between 8 and 16 m horizontally, at depths of about 2.5 to 4.8 m (Fig. 10).

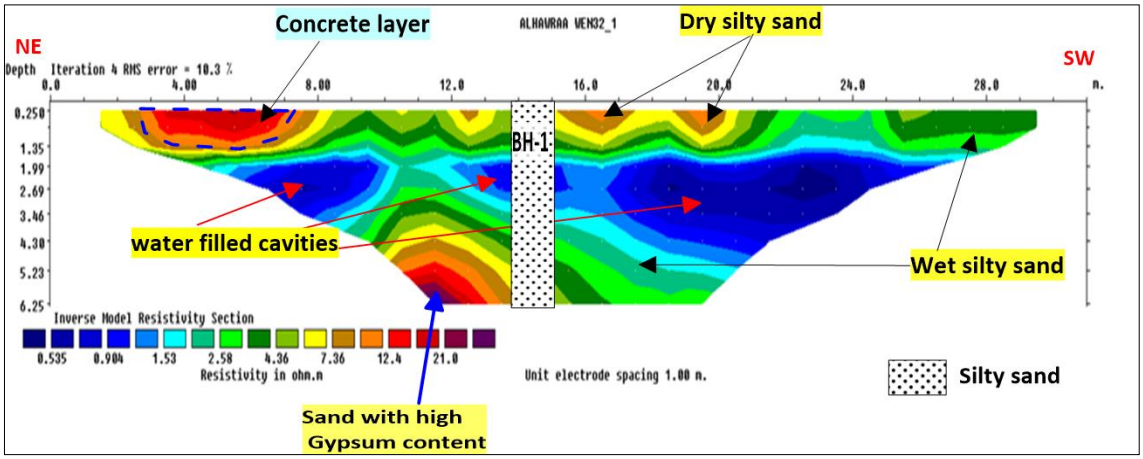

Fig. 9. Inverse models of the synthetic model for the Wenner array of site 2DZ

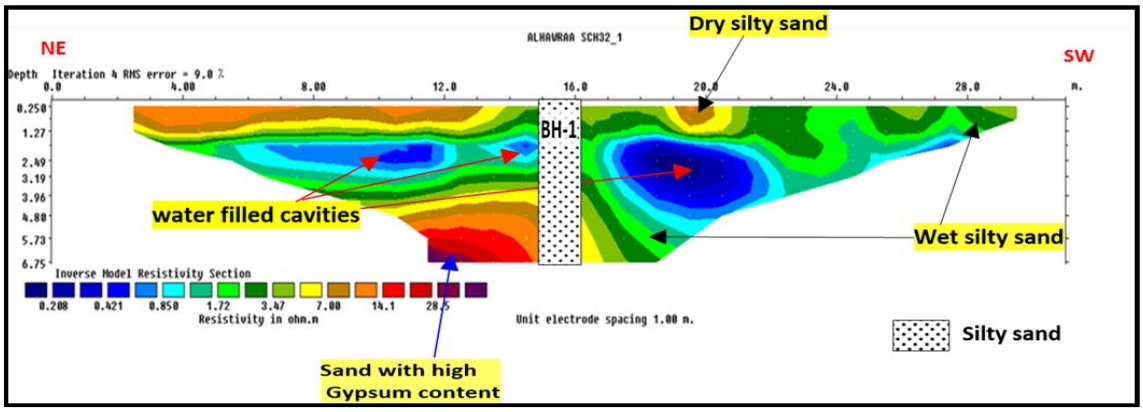

Fig. 10. Inverse models of the synthetic model for the Schlumberger array of site 2DZ.

The site 2DZ (Zain Al-Abideen Street) is characterized by water-filled cavities caused by secondary gypsum dissolution, which weakens the soil and creates underground voids. Wet silty sand was also indicated in places with medium resistivity (between 3.5 and 7 Ωm), particularly in the southwest portion of the profile. Beneath the water-filled voids, high resistivity zones (over 14 Ωm) were discovered; these are thought to be dry sands with a high secondary gypsum concentration. It is also observed that, in contrast to the Wenner and Dipole-Dipole arrays, the surface pavement layer was not readily visible in this part. This is probably because the Schlumberger array concentrates more on vertical variations at deeper depths, making it less sensitive to thin surface layers. Nevertheless, this area mirrored the findings from the other two arrays and assisted in confirming the existence of subterranean weak zones.

4.2.3. Dipole-dipole array

In the resistivity section generated using the Dipole-Dipole array, resistivity values ranged from 0.006 to more than 8 Ωm, showing clear contrasts between different subsurface layers. The very low resistivity zones (between 0.006 and 0.6 Ωm) appeared mainly between 8 and 20 m horizontally, and at depths from about 2 to 5 m (Fig. 11). These zones are thought to be water-filled cavities brought on by the secondary gypsum dissolution, which weakens the soil by creating subsurface cavities. Wet silty sand was found in areas surrounding these cavities with higher resistivity values (about 1 to 2 Ωm). Resistivity values rose beyond 8 Ωm in the center and lower portions of the section, particularly below the water-filled zones, suggesting the existence of dry sand layers with a high secondary gypsum

content. The Dipole-Dipole array was more responsive to lateral movements and displayed higher detail close to the surface than the Schlumberger array. This explains why the borders of weak zones are more distinct and the pavement layer on the surface is more visible.

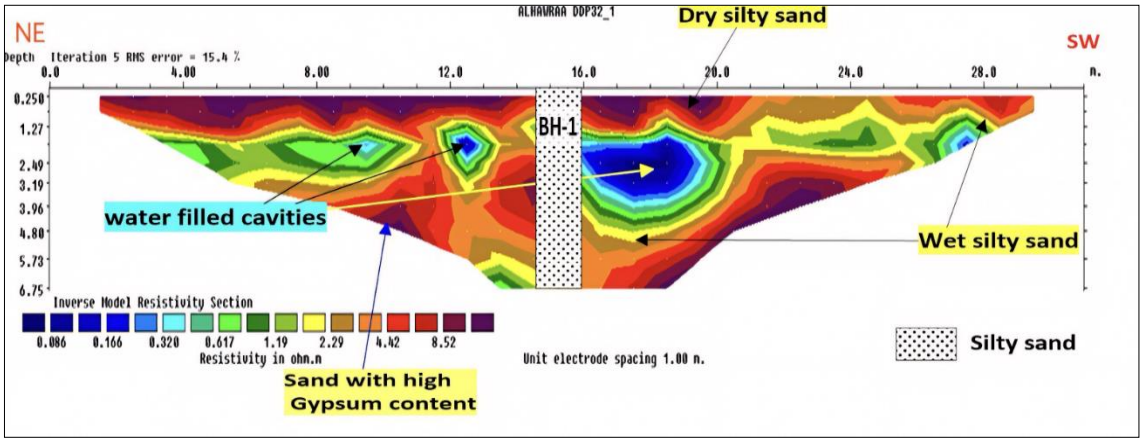

Fig. 11. Inverse models of the synthetic model for the Dipole-Dipole array of site 2DZ

The Dipole-Dipole array is less efficient at deep penetration than the others, but in this instance, its capacity to map horizontal variations and identify shallow cavities made it quite helpful.

5. Discussion

The Electrical Resistivity Imaging (ERT) approach was used in this study to assess subsurface soil conditions and detect probable weak or anomalous zones at two sites inside Al-Najaf City: Al-Ghadeer Village and Zain Al-Abideen Street. Three electrode arrangements, including the Wenner, Schlumberger, and Dipole–Dipole arrays, were employed to ensure comprehensive lateral and vertical characterization of the subsurface layers.

The interpretational dependability at the Al-Ghadeer site was much improved by combining 2D resistivity models with lithological data from boreholes BH-13, BH-15, and BH-16. Saturated and weak soil layers were linked to low-resistivity anomalies (<20 Ωm), while dry sandy layers have high-resistivity values. It was linked to an increase in secondary gypsum. While the Dipole–Dipole arrangement successfully identified lateral heterogeneities suggestive of possible weak zones, the Schlumberger array offered enhanced sensitivity to vertical lithological layering. The inversion data at Zain Al-Abideen Street also showed a substantial association with BH-1's lithological profile.

Higher resistivity values were interpreted as dry sandy soils with likely secondary gypsum content, whereas the Wenner and Schlumberger models showed low-resistivity features clustered toward the section's center, suggesting water buildup or weakly compacted soils. Significant lateral resistivity variation linked to variations in soil compaction and moisture distribution was identified by the Dipole–Dipole model. Complementary benefits were obtained by combining the three electrode configurations: (i) Wenner: improved vertical resolution; (ii) Schlumberger: deeper penetration; and (iii) Dipole–Dipole: efficient imaging of horizontal resistivity differences.

Confidence in the subsurface characterization at both locations was greatly increased by this integration. However, overlapping resistivity signals across various soil types, especially under changeable moisture levels, and the impact of surface noise on shallow-depth resolution in Dipole–Dipole models continue to provide significant challenges for interpretation. Therefore, in order to achieve a more thorough engineering assessment, geophysical results should be accompanied by supplementary geotechnical data.

6. Conclusions

At two distinct locations in Al-Najaf City, the Wenner, Schlumberger, and Dipole-Dipole arrays were used in 2D electrical resistivity tomography (ERT) technology. The resistivity values in the 2D inversion models varied according to the kind and moisture content of the soil. The trustworthiness of the results is supported by the interpretations' good fit with the borehole data (BH-1, BH-13, BH-15, and BH-16). A sharper view of the subsurface was provided, and interpretation mistakes were decreased by using many configurations. Engineers and planners may find this useful when looking at subsidence issues or in upcoming construction projects.

7. Recommendations

More geophysical investigations utilizing 2D and 3D electrical resistivity techniques are advised in order to obtain more precise and lucid pictures of the subsurface, particularly in areas with a high secondary gypsum concentration.

Acknowledgements

I would like to express my gratitude to Al-Mawal Engineering Investigations Company for providing me with the tools and borehole data I needed for this study. I also want to express my gratitude to the technical personnel for their assistance. I also want to express my gratitude to Dr. Amer Al-Khalidi, my supervisor, for his assistance and direction during the project. His advice and encouragement were really helpful and enabled me to complete my course.

References

Abu-Zeid, N., Botteon, D., Cocco, G., Santarato, G., 2006. Non-invasive characterisation of ancient foundations in Venice using the electrical resistivity imaging technique. NDT & E International, 39(1), 67-75. https://doi.org/10.1016/j.ndteint.2005.06.007

Afuwai, C., 2013. Understanding the basics of Electrical Resistivity Geophysical Survey (1st ed.). LAP LAMBERT Academic Publishing.

Al-Farhan, M., Oskooi, B., Abedi, M., Ebrahim Zadeh Ardestani, V., Al-Khalidy, A., 2022. Implications on oil trapping in the Kifl field of Iraq through geophysical investigations. International Journal of Mining and Geo-Engineering, 56(4), 391-400. https://doi.org/10.22059/IJMGE.2022.342321.594971

Al-Farhan, M., Oskooi, B., Ardestani, V.E., Abedi, M., Al-Khalidy, A., 2019. Magnetic and gravity signatures of the Kifl oil field in Iraq. Journal of Petroleum Science and Engineering, 183, 106397. https://doi.org/10.1016/j.petrol.2019.106397

Al-Khalidy, A.A., 2025. Determining soil properties using vertical electrical sounding: The case study of the power electrical station project in Al-Debony, Iraq. Engineering, Technology & Applied Science Research, 15 (3), 23514-23521. https://doi.org/10.48084/etasr.10751

Awadh, S.M., Al-Ankaz, Z.S., Al-Owaidi, M.R., Armstrong-Altrin, J.S., 2024. Provenance and depositional setting of the Late Miocene-Pleistocene clastic sediments in the eastern Arabian Peninsula and western Iraq using rare earth elements geochemistry. Acta Geochimica, 43(2), 399-410. https://doi.org/10.1007/s11631-023-00658-y

Dahlin, T., 1996. 2D resistivity surveying for environmental and engineering applications. First break, 14(7), 1137. https://doi.org/10.3997/1365-2397.1996014

Hussein, M.L., Alattabi, A.N., Al-Owaidi, M.R., Husein, A.A., Altaiand, S., 2022. Petrographic study of Injana Formation in selected areas in Iraq. International Symposium on Multidisciplinary Studies and Innovative Technologies, Ankara, Turkey, 94-104. https://doi.org/10.1109/ISMSIT56059.2022.9932719.

Islam, T., Chik, Z., Mustafa, M.M., Sanusi, H., 2012. Estimation of soil electrical properties in a multilayer earth model with boundary element formulation. Mathematical Problems in Engineering, 2012(1), 472457. https://doi.org/10.1155/2012/472457

Kelly, W.E., 1976. Geoelectric sounding for delineating groundwater contamination. Groundwater, 14(1), 6-10. https://doi.org/10.1111/j.1745-6584.1976.tb03626.x

Loke, M.H., 2021. Tutorial: 2-D and 3-D Electrical Imaging Surveys. http://www.geotomosoft.com.

Mohammed, O.J., Abed, A.M., Alnuaimi, M.A., 2021. Evaluation and delineation of sulfur groundwater leakages using electrical resistivity techniques in Hit Area, Western Iraq. Iraqi Journal of Science, 62(7), 2239–2249. https://doi.org/10.24996/ijs.2021.62.7.13

Nordiana, M.M., Rosli, S., Mokhtar, S.M., Nawawi, N.M., Azwin, I.N., 2012. Imaging subsurface characterization at Bukit Bunuh using 2D resistivity method: The effectiveness of enhancing horizontal resolution (EHR) technique. International Journal of Environmental Science and Development, 3(6), 569-573. https://doi.org/10.7763/IJESD.2012.V3.287

Reynolds, J.M., 2011. An Introduction to Applied and Environmental Geophysics. John Wiley & Sons.

Shakir, A.M., Foti, S., Garofalo, F., Hijab, B.R., Laftah, A.A., 2013. Laterally constrained inversion of surface wave data at Najaf City (Iraq) Soil Dynamics and Earthquake Engineering, 45, 89–95. https://doi.org/10.1016/j.soildyn.2012.11.003

Sissakian, V.K., Fouad, S.F., 2015. Geological map of Iraq, scale 1: 1000 000, 4th Edition, 2012. Iraqi Bulletin of Geology and Mining, 11(1), 9-16.

Telford, W.M., Geldart, L.P., Sheriff, R.E., 1990. Applied Geophysics (2nd Ed.). Cambridge University Press, Cambridge.

Thabit, J.M., Al-Zubedi, A.S., 2015. Evaluation of three important electrode arrays in defining the vertical and horizontal structures in 2D imaging surveys. Iraqi Journal of Science, 56(2B), 1465-1470.